Journal of the American Oil Chemists' Society

Surfactants & Detergents

Technical News feature

Interactions Between Linear Alkylbenzene Sulfonates and Water Hardness Ions. I. Effect of Calcium Ion on Surfactant Solubility and Implications for Detergency Performance[1]

K. LEE MATHESON, MICHAEL F. COX and **DEWEY L. SMITH,** Vista Chemical Company, P.O. Box 500, Ponca City, OK 74602

ABSTRACT

This paper examines the interactions of linear alkylbenzene sulfonate (LAS) surfactants with calcium ions. Calcium sulfonate precipitation boundary diagrams are given which provide a convenient way to study these interactions over a wide range of surfactant and hardness ion levels. Some implications of these interactions for detergency performance are discussed.

INTRODUCTION

The interactions by which water hardness ions decrease detergency performance may be considered to fall into four general categories: (a) hardness-cloth substrate interactions; (b) hardness-soil interactions; (c) hardness-builder interactions, and (d) hardness-surfactant interactions. The detrimental effects of interactions (a), (b) and (c) will occur no matter which surfactant is used in the detergent system (1). The detrimental effects of interaction (d) are widely known to occur with certain anionic surfactants by the precipitation of these surfactants with the water hardness ions. The focus of this paper is to examine the interaction of linear alkylbenzene sulfonate (LAS) surfactants with calcium ions over a range of surfactant and hardness ion levels. In the following two papers, the effects of certain additives to modify the LAS/calcium ion interaction are discussed.

[1]Presented at AOCS meeting in Philadelphia, May 1985.

EXPERIMENTAL

Each of the LAS samples used in this study represented commercially available materials. The carbon-chain distributions for the LAS samples are listed in Table I. The samples were deoiled and desalted.

The calcium/surfactant mixtures used to define the precipitation boundary diagrams were prepared using LAS and reagent grade $CaCl_2$. Observations of turbidity were taken after 24 hr using a .5 MW HeNe laser (Spectra Physics) together with a dark background sample observation box. Mixtures were judged to be clear if no red line indicative of the red HeNe laser beam's path was observed (at an observation angle of 90° to the incident laser beam). Mixtures were judged to be turbid if cloudiness or precipitate was plainly visible or if the red line indicating the laser beam's path was visible at the 90° observation angle.

Solutions of LAS and $CaCl_2$ were prepared at twice the desired concentration so that, after blending 10 ml each of the two solutions, the desired final concentration was achieved. The graphs were displayed on base 10, 4-cycle, log-log paper. To facilitate preparation of the solutions, LAS and Ca^{+2} mixtures were prepared in concentrations at ¼ log unit intervals. By preparing sufficient quantities of each of the four most concentrated stock solutions of LAS and Ca^{+2}, it was possible to prepare all the other mixtures by simple 1 to 10 dilutions.

TABLE I

Analytical Data for Commercial[a] LAS Samples

Average carbon chain	$C_{11.4}$	C_{12}	C_{13}
Average molecular weight LAS	339	343	363
Typical carbon chain distribution			
C_{10}	20	13	–
C_{11}	34	31	2
C_{12}	36	29	22
C_{13}	9	24	48
C_{14}	1	3	28
Typical avg. % 2-phenyl isomer	28.6	14.5	11.5
% active in deoiled, desalted sample	96.3	96.4	97.1

[a]Samples were LAS derivatives of Nalkylene® 500, Nalkylene® 550L, and Nalkylene® 600L alkylates available from Vista Chemicals, Houston, Texas.

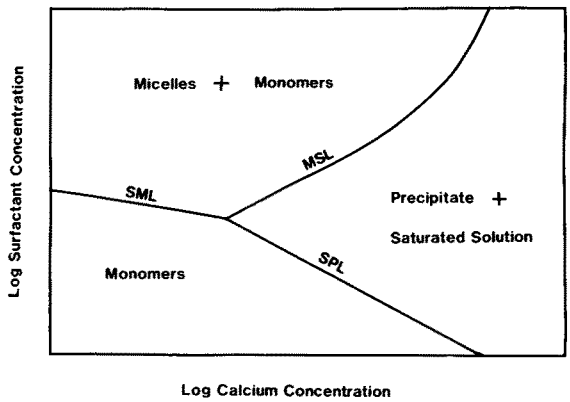

FIG. 1. Generalized calcium sulfonate precipitation boundary diagram.

PRECIPITATION BOUNDARY DIAGRAMS

In order to examine the interactions of LAS with calcium ions over a range of both surfactant and hardness concentrations, precipitation boundary diagrams were constructed. These diagrams provide much useful information about the interaction of anionic surfactants with Ca^{+2} ions. Several articles have appeared in the literature recently which address the subject of precipitation bounday diagrams for Ca^{+2} salts of anionic surfactants (2-5). This diagram is essentially a phase diagram for an anionic surfactant as a function of Ca^{+2} concentration. It is drawn on a log-log plot of anionic surfactant concentration versus Ca^{+2} concentration. The precipitation boundary is the locus of points at which one observes the onset of precipitation.

A generalized diagram of the boundary is shown in Figure 1. A description of the various line segments making up the boundary has been discussed by other researchers, and we follow their presentation here (2,3). Theoretically, the line segment SPL, or surfactant precipitation line, represents the solubility limit of surfactant monomers in the presence of Ca^{+2}. It is a straight line given by the equation:

$$\log [LAS^-] = -\tfrac{1}{2} \log [Ca^{+2}] + \tfrac{1}{2} \log K_{sp} \qquad [1]$$

where K_{sp} is the solubility product for $Ca(LAS)_2$. This is merely the log of the K_{sp} expression:

$$K_{sp} = [Ca^{+2}] [LAS^-]^2 \qquad [2]$$

The factor of $-\frac{1}{2}$ for the slope comes in because there are two surfactant anions per Ca^{+2} cation. The line segment SML, or surfactant micellization line, shows how the CMC of the surfactant changes with Ca^{+2} concentration. It is given by the equation:

$$\log CMC = a - b \log [Ca^{+2}]_t \qquad [3]$$

where a and b are empirically determined constants and $[Ca^{+2}]_t$ is the total concentrate of Ca^{+2} in solution.

The curved line segment MSL is the micelle saturation line. Above this boundary, as surfactant concentration increases, precipitated calcium surfactant is resolubilized by the micelles. Another way to look at it is that the Ca^{+2} ions are electrostatically bound onto the exterior of the micelles, and this boundary represents the Ca^{+2} saturation limit of the micelles. Below this line, $Ca(LAS)_2$ precipitates out of solution. The equation for this curve is a complex expression which incorporates the total concentration of calcium present, either as ions or precipitate, the degree of association of Ca^{+2} with the micelles, and the CMC, which varies with Ca^{+2} concentration. It is derived as follows. The free Ca^{+2} ion concentration is equal to the total Ca^{+2} ions minus those Ca^{+2} ions associated with the micelles. This is written as:

$$[Ca^{+2}] = [Ca^{+2}]_t - \frac{\alpha}{2} ([LAS^-]_t - CMC) \qquad [4]$$

Here the subscript t refers to the total concentration of a species, and α represents the degree of association of Ca^{+2} to the LAS micelles (at complete association $\alpha = 1$). Here the free LAS monomer concentration is assumed to be equal to the CMC which varies according to equation [3].

Another expression for free Ca^{+2} ion can be derived by taking the antilogarithm of equation [3] and assuming that the K_{sp} expression is still a valid relationship between free Ca^{+2} ion and LAS monomer. This yields:

$$[Ca^{+2}] = \frac{K_{sp}}{10^{2a}} [Ca^{+2}]_t 2b \qquad [5]$$

where a and b are the same empirical constants given in equation [3].

By equating both expressions for free Ca^{+2} ions and rearranging, the equation for the micelle saturation line or curve can be obtained.

$$[LAS^-] = ([Ca^{+2}]_t - \frac{K_{sp} [Ca^{++}]_t 2b}{10^{2a}})2/\alpha + CMC$$

The second term on the right-hand side is just the free Ca^{+2} ion concentration as shown in equation [5]. Although not specifically done in this study, experimental determinations of the free Ca^{+2} concentration, of the CMC, and of α would be one way to verify these equations.

The precipitation boundary, consisting of line segments MSL and SPL, divides the graph into regions of clear solutions and cloudy mixtures. Below line segments SML and SPL, only surfactant monomers are present in solution. Above line segments SML and MSL, both micelles and monomers are present. In the region between MSL and SPL, saturated solution exists in equilibrium with the precipitate of the calcium salt of the surfactant.

Precipitation Boundary Diagrams for $Ca(LAS)_2$

Three commercially available LAS samples representing

carbon chain averages of $C_{11.4}$, C_{12} and C_{13} were deoiled and desalted. Using the experimental procedure described earlier, mixtures of LAS and $CaCl_2$ of known concentration were prepared and placed on a log-log grid of [LAS^-] versus [Ca^{+2}].

From these arrays of mixtures, precipitation boundary diagrams were drawn. In drawing the boundaries, the assumption was made that the lower line had an invariant slope of −½. The diagrams for these three LAS samples are shown in Figures 2-4, both with and without .01M Na_2SO_4. The .01M Na_2SO_4 concentration was selected because it corresponds approximately to the ionic strength contribution from the inorganic components in a typical heavy duty powder formulation, assuming a composition of 15% LAS/30% STPP/5% silicate/35% Na_2SO_4 at a use level of .15%.

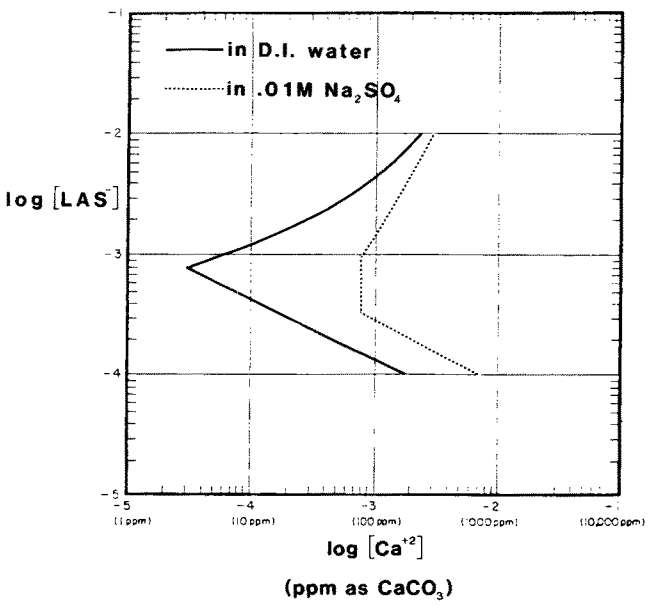

FIG. 2. $Ca(LAS)_2$ precipitation boundary diagrams for $C_{11.4}$ ave. LAS.

The boundary diagrams provide approximate values for the K_{sp} of $Ca(LAS)_2$ and the critical micelle concentration of LAS in the presence of Ca^{+2}. These are shown in Tables II and III. The K_{sp}'s were calculated from the expression $K_{sp} = [Ca^{+2}][LAS^-]^2$ using any point on the linear K_{sp} line of the boundary. The CMC for LAS at 25 C in the presence of Ca^{+2} was taken as the first turning point on the lower half of the boundary. Admittedly, these values must be considered only rough approximations, particularly because the LAS samples consisted of a broad mixture of carbon chain lengths and phenyl isomers.

Using these CMC and K_{sp} values, one can approximate the amounts of free Ca^{+2} ion and micelle-bound Ca^{+2} ion for points on the upper part of the precipitation boundary diagrams. For example, in Figure 4 the point corresponding to 8×10^{-4} M LAS and 10^{-4} M Ca^{+2} lies on the upper part of the boundary diagram for C_{13} average LAS in deionized water. The CMC for this diagram is 2.8×10^{-4} M; therefore, the LAS monomer concentration is roughly 2.8×10^{-4} M, and the amount of LAS in micellar form is 5.2×10^{-4} M. By the K_{sp} expression for this diagram, the amount of free Ca^{+2} ion in equilibrium with 2.8×10^{-4} M LAS monomer is 7.9×10^{-6} M Ca^{+2}. This implies that about 92% of the total 10^{-4} M Ca^{+2} ions at that point are tied up in some fashion with the micellar LAS. The molar ratio of this micelle-bound Ca^{+2} to micellar LAS is about 1 to 5.7.

It could be presumed that some parts of the boundary are determined by single homologs while other regions reflect the combined effects of the carbon chain distribution. For example, the apex and the K_{sp} line probably are determined by the level of the longest carbon chain length homolog, because it is both the most hardness sensitive and the most surface active.

Figures 5 and 6 show superimposed boundaries for the three molecular weight LAS products with and without .01M Na_2SO_4. The carbon chain distributions for these LAS materials are given in Table I. As expected, the heavier molecular weight average LAS shows the greatest sensitivity to precipitation with Ca^{+2}. Both the C_{12} average and the $C_{11.4}$ average LAS show considerably more tolerance to Ca^{+2} than the C_{13} average LAS. This is probably because they contain very little C_{14} LAS homolog and relatively less of the C_{13} LAS homolog.

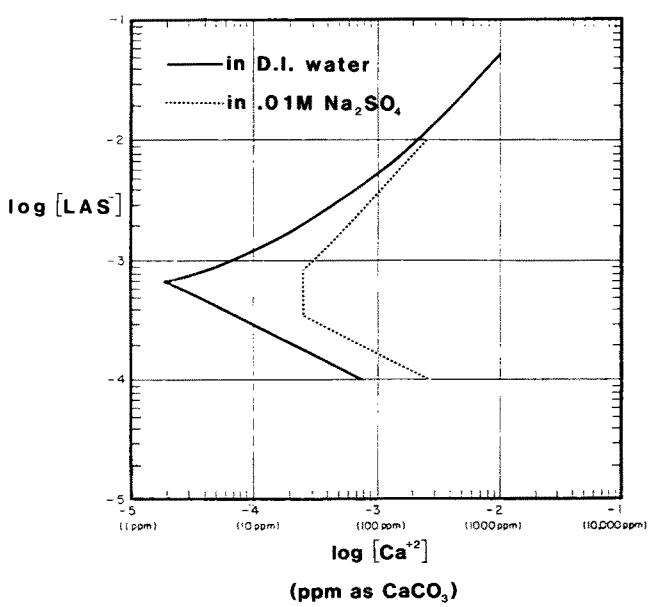

FIG. 3. $Ca(LAS)_2$ precipitation boundary diagrams for C_{12} ave. LAS.

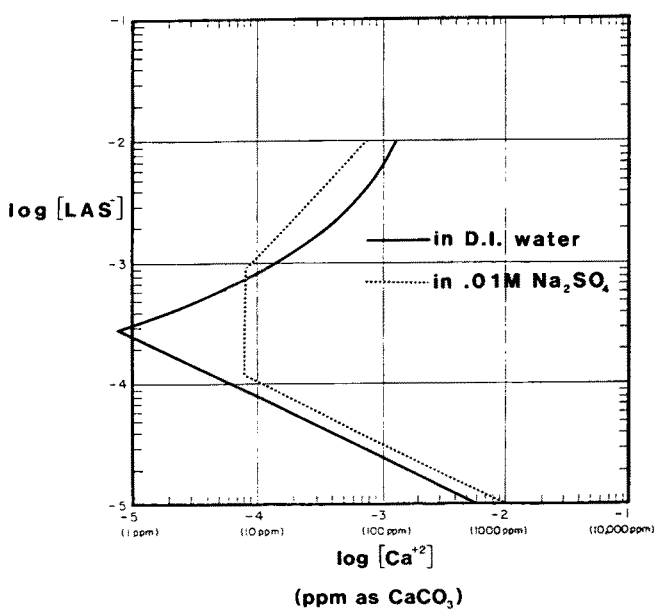

FIG. 4. $Ca(LAS)_2$ precipitation boundary diagrams for C_{13} ave. LAS.

TABLE II

Estimated Values for Commercial[a] LAS Critical Micelle Concentrations in the Presence of Calcium Ion at 25 C

	Estimated CMC's	
LAS avg. M.W.	w/o added salt	In .01M $Na_2^2SO_4$
339 ($\sim C_{11.4}$)	8.5×10^{-4} M	3.3×10^{-4} M
343 ($\sim C_{12}$)	7.0×10^{-4} M	3.1×10^{-4} M
363 ($\sim C_{13}$)	2.8×10^{-4} M	1.2×10^{-4} M

[a]Samples were LAS derivatives of Nalkylene® 500, Nalkylene® 550L, and Nalkylene® 600L alkylates available from Vista Chemicals, Houston, Texas.

TABLE III

Estimated K_{sp} Values for $Ca(LAS)_2$ Using Commercial[a] LAS

	Estimated K_{sp}'s	
LAS avg. M.W.	w/o added salt	In .01M Na_2SO_4
339 ($\sim C_{11.4}$)	1.8×10^{-11}	7.8×10^{-11}
343 ($\sim C_{12}$)	8.4×10^{-12}	2.7×10^{-11}
363 ($\sim C_{13}$)	6.2×10^{-13}	1.0×10^{-12}

[a]Samples were LAS derivatives of Nalkylene® 500, Nalkylene® 550L, and Nalkylene® 600L alkylates available from Vista Chemicals, Houston, Texas.

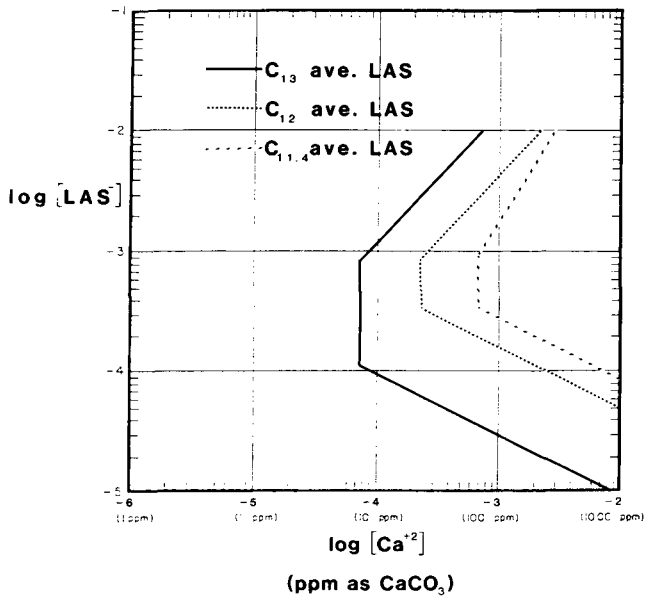

FIG. 6. $Ca(LAS)_2$ precipitation boundary diagrams in .01M Na_2SO_4.

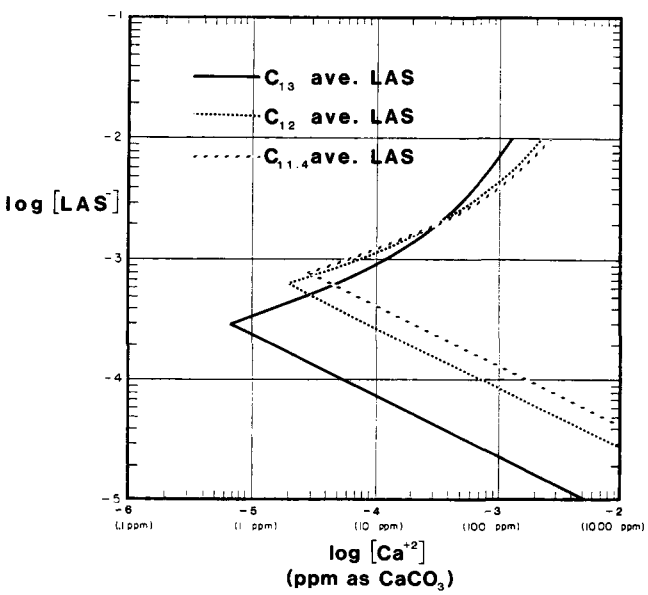

FIG. 5. $Ca(LAS)_2$ precipitation boundary diagrams.

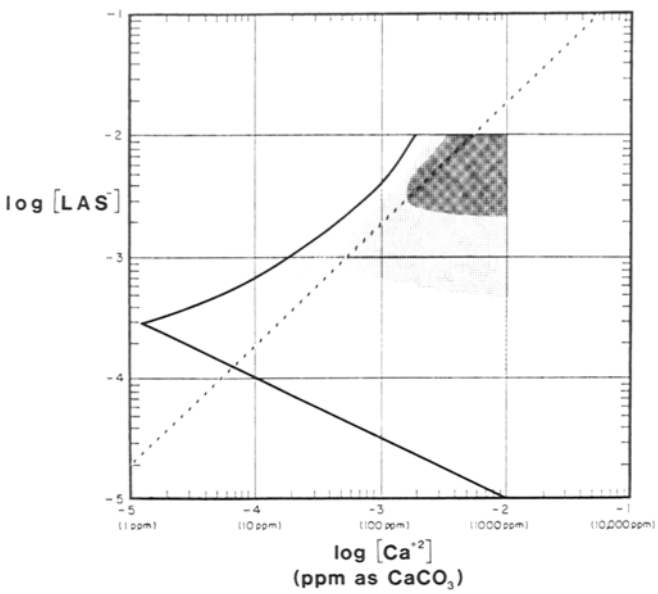

FIG. 7. Generalized diagram showing regions of heavy precipitation.

Although not specifically indicated for any of the grid points on the diagrams, there were some obvious visible differences in the amount of precipitate that formed in any given set of LAS/Ca^{+2} grid mixtures. Mixtures of Ca^{+2} and LAS in the upper right-hand corner of the log-log plot naturally produced the most precipitate. Also, the mixtures within the boundary closer to the line of stoichiometric equivalence (where $[LAS^-] = 2[Ca^{+2}]$) contained more precipitate. A generalized example is shown in Figure 7.

The amount of $Ca(LAS)_2$ precipitate formed in a Ca^{+2}/LAS diagram generally can be approximated for many points within the precipitation boundary by using simple stoichiometric relations and the assumption that one Ca^{+2} ion will combine with two LAS monomers. These approximations can be made using a family of curves given by the expression:

$$10^y = 2(10^x) + 2C$$

where $y = \log [LAS^-]_t$, $x = \log [Ca^{+2}]_t$, and $C = \frac{1}{2}[LAS]_t - [Ca^{+2}]_t$. The derivation of this expression has been described previously (6). The graph of these curves is shown in Figure 8. The term C, which gives rise to the various curves, is itself determined by the initial bulk concentrations of $[Ca^{+2}]$ and $[LAS^-]$. When $[Ca^{+2}]$ is present in stoichiometric excess, C is negative; when $[LAS^-]$ is present in stoichiometric excess, C is positive. If $[LAS^-]$ and $[Ca^{+2}]$ are at stoichiometric equivalence ($[LAS^-] = 2[Ca^{+2}]$), then C = 0.

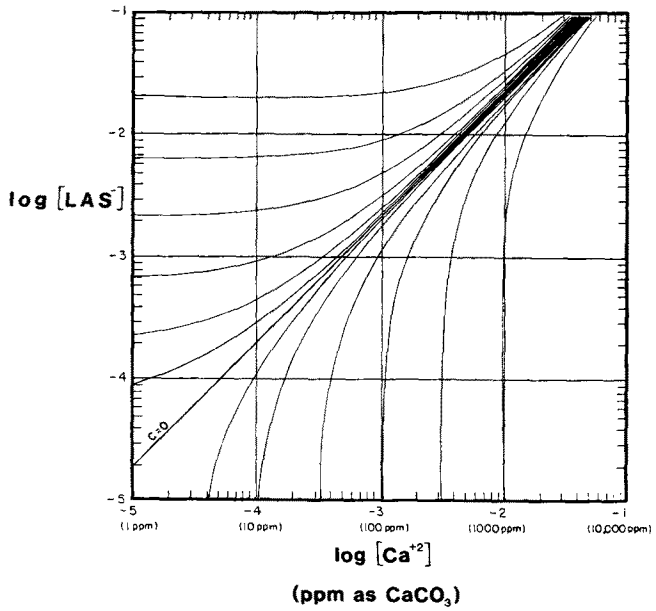

FIG. 8. Family of curves generated by the expression $10^y = 2 \cdot 10^x + 2C$.

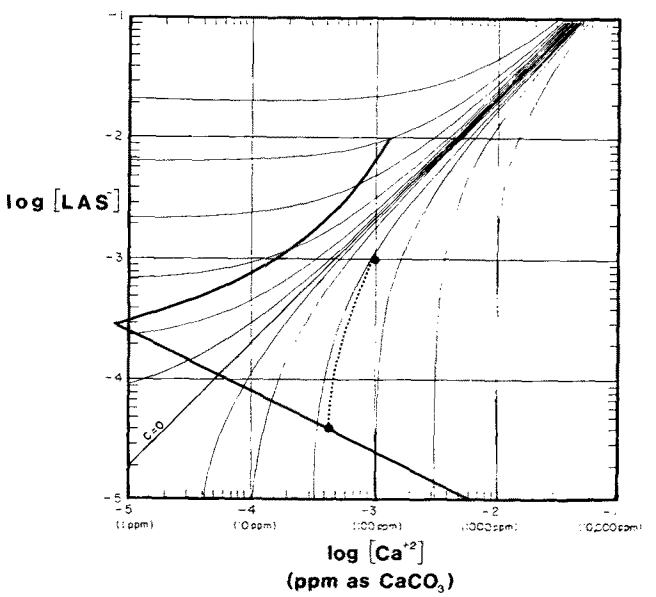

FIG. 9. $Ca(LAS)_2$ precipitation boundary diagram for C_{13} ave. LAS.

It is useful to examine the general characteristics of this family of curves, because on a qualitative basis they help explain some LAS detergency phenomena (6). As shown in Figure 8, the curves on the upper side of the C = 0 line of stoichiometric equivalence curve out toward the log [LAS^-] axis because they represent initial concentrations where [LAS^-] is present in stoichiometric excess. Similarly, the curves on the lower side of the C = 0 line curve down toward the log [Ca^{+2}] axis because they represent initial concentrations where [Ca^{+2}] is present in excess.

Take as an example an initial mixture of 10^{-3} M of the C_{13} average LAS with 10^{-3} M Ca^{+2} as shown in Figure 9. As the $Ca(LAS)_2$ begins to precipitate out, the concentrations of dissolved LAS remaining and of free Ca^{+2} ion will gradually change in a manner parallel to the nearest indicated curve. Equilibrium is reached at the intersection with the precipitation boundary which in this case is the K_{sp} line. As shown in Figure 9, the curve would predict for this Ca^{+2}/LAS mixture an equilibrium concentration of approximately 4×10^{-5} M LAS. In the actual experiment, an MBAS analysis of the clear supernatent solution showed the [LAS^-] to be about 5×10^{-5} M, which is reasonably close to the predicted value.

Most likely, the accuracy of these prediction curves would be greater for precipitation boundary diagrams of isomerically pure anionic surfactants. It must be remembered for the diagrams shown in this study that the commercial LAS samples used were complex mixtures of homologs and isomers.

IMPLICATIONS FOR DETERGENCY PERFORMANCE

The precipitation boundary diagrams provide a quantitative description of the Ca^{++}/LAS^- interactions.

In order to discuss the implications of these boundary diagrams for detergency performance, it is important to place the [Ca^{+2}] and [LAS^-] concentration ranges in the perspective of typical wash conditions. At recommended use levels, surfactant concentrations range from about 100 to 500 ppm active in the wash water. The molar concentration will depend, of course, on the average molecular weight of the surfactant, but for a C_{12} LAS, this will range from about 3×10^{-4} M to 1.5×10^{-3} M. Water hardness can range from 0 to about 300 ppm (as $CaCO_3$) or 0 to 10^{-3} M Ca^{+2}. Figures 2-6 show that the apexes of these LAS precipitation boundaries generally lie within the range of interest for typical use conditions.

It is obvious by comparing Figures 3 and 4 why STPP is generally the preferred builder for use with C_{13} average LAS, whereas carbonate frequently is used with heavy-duty powder formulations containing C_{12} average LAS. The increased hardness tolerance of the C_{12} average LAS permits the use of a less effective builder.

When comparing a precipitation boundary diagram of a surfactant to the detergency performance for the real detergent system containing builder, it is important to keep in mind that on the x axis, [Ca^{+2}] should represent the residual unsequestered [Ca^{+2}]. The increased ionic strength due to the presence of builder will change the shape of the boundaries, as shown in Figures 2-4.

It can be observed that with gradually increasing hardness, detergency performance begins to decrease at levels beyond the precipitation boundary. The loss of surfactant (at equilibrium conditions) due to precipitation can be estimated using the curves in Figure 8. Although the kinetics of $Ca(LAS)_2$ formation may not be rapid enough for precipitation to be complete in 10 min, they appear to be fast enough to cause a significant loss of surfactant. The loss of surfactant becomes much more severe as the level of residual [Ca^{+2}] crosses the line of stoichiometric equivalence, as indicated in Figure 9. At typical use concentration of 225 ppm surfactant for an LAS-based heavy-duty powder, this level of residual Ca^{+2} is about 32 ppm. At this point, the predictor curves begin to point down toward the lower boundary. Loss of surfactant by precipitation is more severe because the equilibrium solution concentrations of [Ca^{+2}] and [LAS^-] will lie along the lower boundary or K_{sp} line.

If one compares the detergency performance of an LAS-based formulation as a function of [Ca^{+2}], the most abrupt decrease in detergency coincides roughly with the region where residual [Ca^{+2}] level is slightly greater than about 32 ppm.

Figure 10 shows detergency performance of a C_{13} average LAS-based HDP containing 25% STPP at a use level of .15%. Because this amount of STPP will sequester

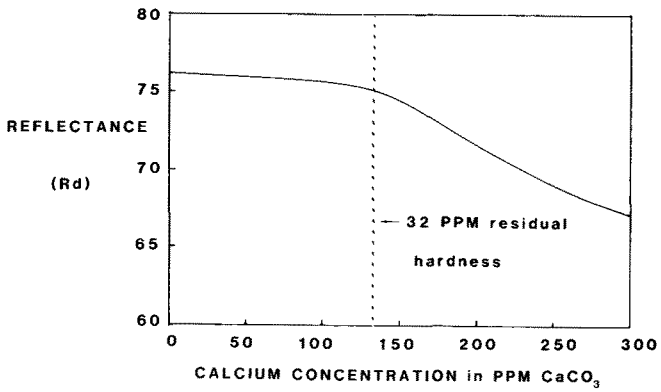

FIG. 10. Detergency performance of C_{13} ave. LAS in 15% LAS/25% STPP/10% silicate/35% Na_2SO_4, 100 F, .15% conc., sebum on cotton.

about 100 ppm hardness, the performance drop-off which starts at about 135 ppm Ca^{+2} hardness does coincide with about 32 ppm residual $[Ca^{+2}]$.

These data confirm the widely held belief that at under-use concentrations, the detergency performance can suffer. The reduced level of surfactant plays a minor role. The major effect is an increase in residual Ca^{+2} resulting from a decrease in builder level. This could now put the initial $[LAS^-]$ and $[Ca^{+2}]$ concentrations beyond the line of stoichiometric equivalence where $[Ca^{+2}]$ ion is in excess and the loss of surfactant by precipitation is much greater. The Ca^{+2}/LAS precipitation boundary diagrams provide a systematic way to study and evaluate the interactions of Ca^{+2} and LAS. Although the diagrams are based on experimental observations after the Ca^{+2}/LAS system has reached equilibrium conditions, some conclusions can be drawn which apply to detergency performance during the ten-minute wash time scale. In the following two papers, we will discuss how certain additives can moderate the Ca^{+2}/LAS interaction to alleviate the deleterious effect of precipitation.

REFERENCES

1. Hollingsworth, M.W., JAOCS 55:49 (1978).
2. Peacock, J.M., and E. Matijevic, J. Colloid Interface Sci. 77:548 (1980).
3. Walker, R.D., et al., "Salting-Out and Multivalent Cation Precipitation of Anionic Surfactants," presented at 181st ACS National Meeting, Atlanta, March 1981.
4. O'Brien, E.F., and B.H. Wiers, Preprints, 48th National Colloid Symposium, 220 (1974).
5. Celik, M.S., E.D. Maney and P. Somasundaran, AIChE Symposium Series 78:86 (1982).
6. Matheson, K.L., JAOCS 62:1269 (1985).

Interactions Between Linear Alkylbenzene Sulfonates and Water Hardness Ions. II. Reducing Hardness Sensitivity by the Addition of Micelle Promotion Agents[1]

MICHAEL F. COX and **K. LEE MATHESON**, Vista Chemical Company, P.O. Box 500, Ponca City, OK 74602

ABSTRACT

Agents which promote micellization of linear alkylbenzene sulfonates (LAS) improve LAS hard-water detergency performance by reducing water hardness sensitivity. A model is proposed which correlates micellization and water hardness tolerance. The ability of inorganic salts and cosurfactants to act as micelle promotion agents is discussed.

INTRODUCTION

As discussed in paper I (1), linear alkylbenzene sulfonates (LAS) interact with free calcium ions to form insoluble $Ca(LAS)_2$. Formation of these complexes reduces the concentration of surfactant available for detergency. Several methods are available for minimizing the effect of this interaction. The most common involves the use of builders to reduce the concentration of water hardness ions. Another is to add more surfactant to make up for the amount lost in the formation of insoluble complexes. A third method, which is the subject of this paper, involves the use of micelle promotion agents to reduce the extent of interaction by effectively lowering the concentrations of both surfactant monomer and water hardness ions.

[1] Presented at the AOCS meeting in Philadelphia, May 1985.

EXPERIMENTAL

Detergency Testing

Detergency tests were performed using the materials and procedures outlined in Table I. All tests were performed in duplicate. Performance was determined by measuring reflectance (in Rd units) of the washed cloths.

TABLE I

Detergency Test Materials and Procedures

Testing apparatus	Terg-O-Tometer
Wash cycle	10 min
Rinse cycle	5 min
Wash temperature	100 F (38 C)
No. soiled cloths	6 (3 cotton, 3 p.press)
No. unsoiled cloths	3 (cotton)
Soil	Sebum
Cotton cloth	Test Fabrics S/419
P.Press cloth	Test Fabrics S/7406 (65% Dacron/35% Cotton)
Formulation use level	0.15%
Test procedure	Vista CRS 303-74[a]
Reflectance measuring device	Gardner (Model XL20) Colorimeter

[a]Similar to ASTM Standards, Part 30, 465-466 (1977).